ヒトにおいても人工内耳施行例でメチルプレドニゾロンの静注と鼓室内注入で鼓室階外リンパ移行濃度を比較した報告がなされており，動物実験と同様に静注投与の 126 倍と高い移行が確認されている[4]。報告により異なるが，投与後 1〜3 時間後で移行したステロイドの濃度はピーク値に達し，そのあとは低下する。抗デキサメタゾン抗体を用いて糖質コルチコイドレセプターの免疫染色を行い，マウス蝸牛内の分布を経時的に調べた報告によると，鼓室内注入後 60 分に移行濃度はピークに達し，全回転のラセン靭帯，基底板，コルチ器，ラセン神経節が濃染することが明らかにされている[5]。したがって，正円窓膜を介して基底回転鼓室階に移行したステロイドは，鼓室階から前庭階・中央階へ，基底回転から頂回転へと拡散し，全回転のコルチ器に到達するといえる。また，鼓室内に注入するステロイドは濃度が高いほど免疫染色で濃染することが報告されており[6]，注入するステロイドの濃度は高いほうが移行はよい。

原因が明らかな急性感音難聴

1 手術による内耳障害

中耳手術の手術操作により内耳障害を生じた場合，医原性の急性感音難聴をきたす。内耳障害を生じえる主な手術操作として真珠腫中耳炎の迷路瘻孔処理や耳硬化症のアブミ骨底板開窓などが挙げられる。迷路瘻孔処理の際のステロイドの内耳保護効果について局所投与で検討した報告はみられないが，術中のステロイド静注の効果に関しては，後ろ向き研究[7,8]で内耳機能の温存に有効なことが報告されている。ただ，無作為比較試験はないため，十分なエビデンスがあるとはいいがたい。また，耳硬化症においても古くから内耳障害の低減，予防を目的としたステロイドの全身投与が行われてきた[9]。しかし，Riechelmann ら[10]は 95 例の耳硬化症を対象として，ステロイド局所投与群，非投与群の術後聴力を比較した無作為比較試験を行った結果，明らかな保護効果は認められなかったと報告している。この報告のほかに無作為比較試験はなく，耳硬化症におけるステロイド局所投与の有効性についても十分なエビデンスは得られていない。

一方，近年低音部に残存聴力を有する高度感音難聴に対して，残存聴力を活用した人工内耳（electric and acoustic stimulation：EAS）手術が行われるようになってきた[11]。当初は内耳の開窓，電極挿入により内耳機能は保存しえないとみなされていたが，残存聴力の保存される例が多く報告されるようになり，保存率の向上を目的とした低侵襲な手術手技とそのための新たな電極が開発されるに至った。低侵襲な手術手技として正円窓経由の電極挿入が行われるが，同時に残存する内耳機能の温存を目的としたステロイドの局所投与[12]も広く行われている。電極挿入に伴う内耳の器械的損傷に対するステロイドの効果の機序は，急性音響外傷と同様に炎症性サイトカインの抑制によるものと考えられている[13]。局所投与の有効性についてヒトを対象とした無作為比較試験は行われていないが，電極挿入による内耳への手術侵襲に対するステロイド局所投与の効果はモルモットを用いた動物実験で確認されている[13]。

2 耳毒性薬物

抗悪性腫瘍薬であるシスプラチンの耳毒性はよく知られており，容量依存性に非可逆性の内耳障害をきたす。耳毒性の発現率は 75〜100％と高く[14]，耳毒性の低減を目的としたさまざまな基礎実験の報告がみられる。現在，シスプラチンによる耳毒性発現の機序は内耳における活性酸素種の産生増加を介した細胞障害，細胞死（アポトーシス）によるものと考えられている。最も障害を受けやすい部位は基底回転外有毛細胞であるため，通常高音漸傾型の感音難聴を示す。活性酸素種の増加が原因となっていることから，抗酸化作用を有する薬物はシスプラチンの耳毒性を軽減し得る。ステロイドも抗酸化作用を有する薬剤の 1 つであり，ステロイドの鼓室内注入により実験的には耳毒性が軽減されることが示されている[15,16]。

アミノ配糖体系抗菌薬による聴覚障害はシスプラチンと同様に非可逆性で，主な障害部位は外有毛細胞である。本薬剤による耳毒性発現の機序は

アミノ配糖体系抗菌薬が鉄キレートとして作用し，内耳における活性酸素種の産生を促進するためと考えられている。したがってシスプラチンと同様に抗酸化作用を有するステロイドには一定の効果があるものと予測される。アミノ配糖体系抗菌薬の耳毒性低減を目的としたステロイド局所投与の効果に関する報告は少ないが，モルモットを用いた動物実験で機能的にも形態的にも内耳障害を低減し得ることが報告されている[17]。

3 細菌性髄膜炎

インフルエンザ菌b型ワクチン（Hibワクチン）が導入されて以降，細菌性髄膜炎の起炎菌としては肺炎球菌が最も頻度が高くなっている。肺炎球菌による細菌性髄膜炎は早期に診断され抗菌薬投与が行われても，後遺症として約1/3に感音難聴を生ずることが知られている[18]。髄膜炎に起因する難聴の機序は髄膜から内耳へ感染，炎症が波及し，細菌性内耳炎をきたすためと考えられている。また，動物実験で非可逆的な感音難聴は蝸牛の炎症やラセン神経節細胞の障害の程度とよく相関することが明らかにされている。細菌性髄膜炎の治療の主体は起炎菌に感受性をもつ抗菌薬の投与であるが，ステロイドは炎症性サイトカインの発現を抑制し，抗炎症作用を有することから難聴の軽減を目的とした抗菌薬とステロイドの併用投与が広く行われている。ステロイドと抗菌薬の併用投与による予防効果については確認できないとする報告もみられるが，メタアナリシスでは細菌性髄膜炎による高度難聴の発症を減少させる効果があるとされている[19]。ステロイドの投与法はすべて全身投与であり，まだ鼓室内投与による効果を検討した臨床試験は報告されていない。しかし，実験的肺炎球菌性髄膜炎ラットを用いて，抗菌薬＋ベタメタゾン鼓室内注入群と抗菌薬＋生理食塩水鼓室内注入群で歪成分耳音響放射（DPOAE），聴性脳幹反応（ABR），ラセン神経節細胞数を比較した報告があり，ラセン神経節細胞の減少を抑制する効果を認めているが，ABRの比較では両群間に差を認めていない[20]。

原因不明の急性感音難聴

1 突発性難聴

原因の不明な急性感音難聴の代表的疾患である突発性難聴の治療には主にステロイドが用いられる。その根拠となっているのが，Wilsonら[21]による無投薬対照とステロイド投与群との二重盲検無作為比較試験であるが，その後Cinamonら[22]は同様な二重盲検無作為比較試験を行っているが有効性を認めていない。そのため，Cochrane reviewではステロイドの有効性については明らかではないと結論している。無投薬群を対照とした無作為比較試験はこの2編のみで，ほかのメタアナリシスにおいても，この2つの報告は症例数が少なく，信頼性に乏しいことが指摘されている。したがって，突発性難聴に対するステロイドの有効性は確かなものとはいえないため，米国における突発性難聴診療ガイドラインではステロイドの初期治療をrecommendationではなくoptionとしている[23]。

一方，鼓室内投与についてみると，ステロイド全身投与無効例に対する救済治療，糖尿病など全身投与の困難例の初期治療，単独での初期治療などさまざまな報告があるが，偽薬を用いた無作為比較試験は初期治療，救済治療それぞれ1報告，計2報告のみである[24,25]。いずれもステロイド鼓室内注入の成績は良好としているが，最新のシステマチックレビューによれば，症例数が少ないためエビデンスとしてはまだ不十分であり，評価としては，①初期治療では全身投与と同等の有効性を有する，②救済治療では13.3 dBの有意の改善（メタアナリシス）を認めるが，この聴力改善が臨床的に意義をもつかは不明，としている[26]。また，2011年にはステロイドの経口投与と鼓室内投与の前向き無作為比較試験の結果が報告された[27]。この比較試験は16施設の参加施設から登録された250例を対象として，経口投与121例（プレドニゾロン60 mg，2週間内服）と鼓室内投与129例（メチルプレドニゾロン40 mg，4回/2週）で治療成績を比較したものである。結果は両群の治療成績に有意差はなく，鼓室内投与の非劣性が示された。結論として，非侵襲的かつコストが安価

で患者にとって治療を受けやすい経口投与のほうが優れており，鼓室内注入は経口内服ができない場合に選択すべきとしている。しかし，2012年に公表された米国の診療ガイドラインでは救済治療としてステロイドの鼓室内注入をrecommendationとした[23]。その根拠として，無作為比較試験以外の報告も含めて，多数の報告で一定してある程度の聴力改善が得られていることを挙げている。投与時期は初期治療終了後，直ちに開始し，3〜7日間隔で3〜4回行うことを推奨している。また，投与法についてはステロイドの種類は高容量デキサメタゾンないしメチルプレドニゾロンを用い，0.4〜0.8 mLを鼓室内に注入した後患側耳を上にした体位を15〜30分維持するように明記している。

メニエール病

メニエール病におけるステロイド鼓室内注入療法についても少ないながら2編の無作為比較試験の報告がある。めまい発作に関しては症例数が22例と少ないが無作為比較試験で有意な抑制効果が報告されている[28]。一方，聴力，耳鳴に対する改善効果はないとされている[29]。

おわりに

近年，ステロイドの鼓室内注入療法は注目されつつあるが，偽薬を用いた無作為比較試験の報告はわずかで，まだ最適な投与量，投与回数，信頼しえる有効性のエビデンスなどいずれも不足している。したがって，現時点で正しい使い方を示すのは困難であるが，少ない投与量で内耳に高濃度のステロイドを投与するには最適の手法であるのは間違いない。その意味でステロイドの鼓室内投与は今後の発展が期待しえる投与法といえる。

文献

1) 野村恭也：蝸牛窓に関する研究．日耳鼻 85：1412-1424，1982
2) 佐藤宏昭：鼓室内注入による内耳へのステロイド移行に関する基礎研究．Otol Jpn 21：157-160，2011
3) 佐藤宏昭・他：CMCステロイドの中耳より内耳への移行．耳鼻臨床 82：715-718，1989
4) Bird PA, et al：Intratympanic versus intravenous delivery of methylprednisolone to cochlear perilymph. Otol Neurotol 28：1124-1130, 2007
5) Hargunani CA, et al：Intratympanic injection of dexamethasone：time course of inner ear distribution and conversion to its active form. Otol Neurotol 27：564-569, 2006
6) Fu Y, et al：Intratympanic dexamethasone as initial therapy for idiopathic sudden sensorineural hearing loss：clinical evaluation and laboratory investigation. Auris Nasus Larynx 38：165-171, 2011
7) Dornhoffer JL, et al：Management of the open labyrinth. Otolaryngol Head Neck Surg 112：410-414, 1995
8) Gocea A, et al：Preserving bone conduction in patients with labyrinthine fistula. Eur Arch Otorhinolarungol 269：1085-1090, 2012
9) Shambaugh GE, et al：New concepts of management of otospongiosis. Arch Otolaryngol 100：419-426, 1974
10) Riechelmann H, et al：Perioperative glucocorticoid treatment does not influence early post-laser stapedectomy hearing thresholds. Am J Otol 21：809-812, 2000
11) von Ilberg C, et al：Electric-acoustic stimulation of the auditory system. ORL J Otorhinolaryngol Relat Spec 61：334-340, 1999
12) Rajan GP, et al：The role of preoperative, intratympanic glucocorticoids for hearing preservation in cochlear implantation：a prospective clinical study. Laryngoscope 122：190-195, 2012
13) Eshraghi AA, et al：Local dexamethasone therapy conserves hearing in an animal model of electrode insertion trauma-induced hearing loss. Otol Neurotol 28：842-849, 2007
14) McKeage MJ：Comparative adverse effect profiles of platinum drugs. Drug Saf 13：228-244, 1995
15) Daldal A, et al：The protective effect of intratympanic dexamethasone on cisplatin-induced ototoxicity in guinea pigs. Otolaryngol Head Neck Surg 137：747-752, 2007
16) Hill GW, et al：Cisplatin-induced ototoxicity：effect of intratympanic dexamethasone injections. Otol Neurotol 29：1005-1011, 2008
17) Himeno C, et al：Intra-cochlear administration of dexamethasone attenuates aminoglycoside ototoxicity in the guinea pig. Hear Res 167：61-67, 2002
18) Weisfelt M, et al：Dexamethasone and long-term outcome in adults with bacterial meningitis. Ann Neurol 60：456-468, 2006
19) Brouwer, et al：Corticosteroids for acute bacterial meningitis. Cochrane Database Syst Rev CD004405, 2013
20) Worsoe L, et al：Intratympanic steroid prevents long-term spiral ganglion neuron loss in experimental meningitis. Otol Neurotol 31：394-403, 2010
21) Wilson WR, et al：The efficacy of steroids in the treatment of idiopathic sudden hearing loss. A double-blind clinical study. Arch Otolaryngol 106：772-776, 1980
22) Cinamon U, et al：Steroids, carbogen or placebo for sudden hearing loss：a prospective double-blind study. Eur Arch Otorhinolaryngol 258：477-480, 2001
23) Stachler RJ, et al：Clinical practice guideline：sudden hearing loss. Otolaryngol Head Neck Surg146 (3 Suppl)：SI-35, 2012

24) Battaglia A, et al：Combination therapy (intratympanic dexamethasone＋hig-dose prednisone taper) for the treatment of idiopathic sudden sensorineural hearing loss. Otol Neurotol 29：453-460, 2008
25) Plonkte SK, et al：Randomized, double blind, placebo controlled trial on the safety and efficacy of continuous intratympanic dexamethasone delivered via a round window catheter for severe to profound sudden s idiopathic sensorineural hearing loss after failure of systemic therapy. Laryngoscope 119：359-369, 2009
26) Spear SA, et al：Intratympanic steroids for sudden sensorineural hearing loss：a systemic review. Otolaryngol Head Neck Surg 145：534-543, 2011
27) Rauch SD, et al：Oral vs intratympanic corticosteroid therapy for idiopathic sudden sensorineural hearing loss. JAMA 305：2071-2079, 2011
28) Garduno-Anaya MA, et al：Dexamethasone inner ear perfusion by intratympanic injection in unilateral Meniere's disease：a two-year prospective, placebo-controlled, double-blind, randomized trial. Otolaryngol Head Neck Surg 133：285-294, 2005
29) Silverstein H, et al：Dexamethasone inner ear perfusion for the treatment of Meniere's disease：a prospective randomized, double-blind, crossover trial. Am J Otol 19：196-201, 1998

Otolaryngology -- Head and Neck Surgery
http://oto.sagepub.com/

Labyrinthine Artery Detection in Patients with Idiopathic Sudden Sensorineural Hearing Loss by 7-T MRI

Hiroaki Sato and Kazuaki Kawagishi

Otolaryngology -- Head and Neck Surgery published online 31 December 2013
DOI: 10.1177/0194599813517990

The online version of this article can be found at:
http://oto.sagepub.com/content/early/2013/12/30/0194599813517990

Published by:
SAGE
http://www.sagepublications.com

On behalf of:
AMERICAN ACADEMY OF OTOLARYNGOLOGY-- HEAD AND NECK SURGERY
FOUNDATION
American Academy of Otolaryngology- Head and Neck Surgery

Original Research

AMERICAN ACADEMY OF OTOLARYNGOLOGY–HEAD AND NECK SURGERY FOUNDATION

Otolaryngology–Head and Neck Surgery
201X, Vol XX(X) 1–5

DOI: 10.1177/0194599813517990
http://otojournal.org
SAGE

Labyrinthine Artery Detection in Patients with Idiopathic Sudden Sensorineural Hearing Loss by 7-T MRI

Hiroaki Sato, MD, PhD[1], and Kazuaki Kawagishi, MD[1]

Sponsorships or competing interests that may be relevant to content are disclosed at the end of this article.

Abstract

Objective. To compare the detection rates of the labyrinthine artery in subjects with idiopathic sudden sensorineural hearing loss (ISSHL) and in normal-hearing controls using 7-T magnetic resonance imaging (MRI).

Study Design. Cross-sectional study.

Setting. Tertiary referral center.

Subjects and Methods. In 18 patients (9 males, 9 females) with ISSHL and 32 volunteers (21 males, 11 females) with normal hearing, 7-T MRI (Discovery MR950; GE Healthcare, Milwaukee, Wisconsin) was performed with the 3-dimensional time-of-flight spoiled gradient echo (3D TOF SPGR) sequence to compare the detection rates of the labyrinthine artery.

Results. The MRI scans were performed from 3 to 54 days after onset. Of the 18 patients with ISSHL, 8 showed complete recovery, 9 showed partial recovery, and the rest showed no recovery. The labyrinthine artery was depicted in 36 of 36 ears (100%) in the ISSHL group and 63 of 64 (98.4%) ears in the normal-hearing group, with no significant difference in detection rates.

Conclusion. To our knowledge, the present study is the first to report depiction of the labyrinthine artery by 7-T MRI. These preliminary results indicate occlusion of the labyrinthine artery would be rare in the pathogenesis of ISSHL, and they also demonstrate that the labyrinthine artery could be detected by ultra-high-field MRI.

Keywords

labyrinthine artery, 7-T MRI, idiopathic sudden sensorineural hearing loss

Received September 23, 2013; revised November 21, 2013; accepted December 4, 2013.

The pathogenesis of idiopathic sudden sensorineural hearing loss (ISSHL) is still unknown, but an inner ear circulatory disturbance has been considered one possible pathogenesis, comparable to cardiovascular diseases such as stroke or myocardial infarction. A recent meta-analysis of the cardiovascular risk factors for ISSHL indicated a positive association between cardiovascular risk factors and ISSHL.[1] It is also well known that the inner ear can be infarcted in patients with anterior inferior cerebellar artery (AICA) stroke, because the labyrinthine artery, which usually branches from the AICA, is an end artery.[2-4] Cases of labyrinthine infarction secondary to AICA occlusion are often accompanied by clinical symptoms other than hearing loss, including Horner's syndrome, diplopia, ipsilateral facial weakness, vertigo, and ataxia.[4] However, AICA infarction[5] and labyrinthine artery infarction[6] exhibiting only deafness and vertigo have also been reported, although rarely.

The labyrinthine artery is very difficult to depict due to its small diameter.[7,8] However, ultra-high-field magnetic resonance imaging (MRI), such as 7-T MRI, may have the potential to detect the labyrinthine artery because of its high signal-to-noise ratio, being able to provide fine images with the resolution of a few hundred microns. In the present study, depiction of the labyrinthine artery was attempted using 7-T MRI with the 3-dimensional (3D) time-of-flight spoiled gradient echo (3D TOF SPGR) sequence, and the detection rates were compared between normal-hearing controls and patients with ISSHL.

Subjects and Methods

Subjects

This study included 19 consecutive patients with ISSHL (male-to-female ratio of 9:10; age range, 25-75 years; mean [SD] age, 53.2 [17.0] years) and 32 normal-hearing controls without a history of hearing impairment (male-to-female ratio of 8:6; age range, 21-55 years; mean [SD] age, 27.6

[1]Department of Otolaryngology–Head & Neck Surgery, Iwate Medical University, Morioka, Iwate, Japan

This article was presented at the 2013 AAO-HNSF Annual Meeting & OTO EXPO; September 29–October 2, 2013; Vancouver, British Columbia, Canada.

Corresponding Author:
Hiroaki Sato, MD, PhD, Department of Otolaryngology–Head & Neck Surgery, Iwate Medical University, School of Medicine, 19-1 Uchimaru, Morioka, Iwate 020-0805, Japan.
Email: hisato@iwate-med.ac.jp

Table 1. Criteria for the diagnosis of idiopathic sudden sensorineural hearing loss.

Main symptoms
1. Sudden onset of hearing loss; patient can say clearly when it appeared
2. Sensorineural hearing loss, usually severe
3. Unknown cause
Accessory symptoms
1. May be accompanied by tinnitus
2. May be accompanied by vertigo, nausea, and/or vomiting without recurrent episodes
3. No cranial nerve symptoms other than from the eighth nerve
Definite: all the above criteria
Probable: main symptoms 1 and 2

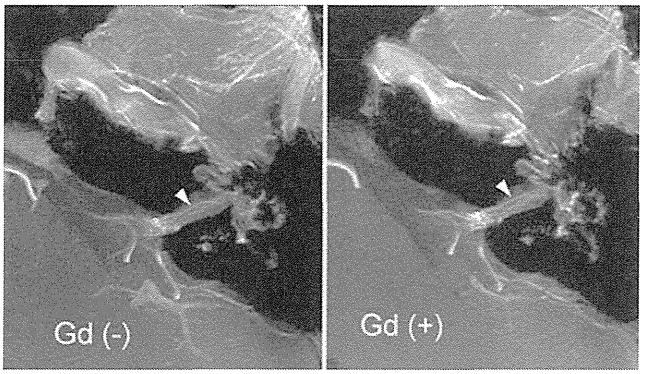

Figure 1. Comparison of magnetic resonance (MR) images of the labyrinthine artery with and without gadodiamide (Gd) enhancement (left ear of a 30-year-old man, normal control; case 2). The labyrinthine artery (arrowhead) can be clearly depicted on MR images with (right) and without (left) Gd enhancement.

[6.7] years). The diagnosis of ISSHL was based on the criteria of the Sudden Deafness Research Committee of the Japanese Ministry of Health, Labor and Welfare (**Table 1**). All subjects met the audiometric hearing criteria of more than 30 dB affecting at least 3 consecutive frequencies.[9] Hearing level was defined as a pure-tone average (PTA) of 0.25, 0.5, 1, 2, and 4 kHz. One patient (65-year-old woman) with ISSHL was excluded from this study because evaluation of the labyrinthine artery was not possible due to motion artifact. Therefore, 18 patients with ISSHL and 32 normal-hearing controls were enrolled in the present study.

All patients with ISSHL were given oral administration of corticosteroid (betamethasone 4 mg with tapering), vitamin B_{12}, and adenosine triphosphate for 12 days, as well as intravenous administration of low-molecular-weight dextran for 5 days. Hyperbaric oxygen therapy was used simultaneously for 11 of 18 patients with ISSHL.

Hearing Level Evaluation

Hearing levels were evaluated at the initial and final visits. The final visit varied from 3 to 231 days (mean [SD], 94.3 [97.0] days) from onset. When the patients did not respond to the maximum sound level generated by the audiometer, the threshold was defined as 5 dB more than the maximum level. Recovery was classified into 3 categories: complete (PTA within 10 dB of the initial hearing level or within 10 dB of the hearing level of the unaffected ear), partial (PTA within 50% of the initial hearing level or >10-dB improvement of the hearing level), and no recovery (<10-dB improvement relative to the initial hearing level).[9]

Scan Parameters of MRI

A 7-T MRI scanner (Discovery MR950: GE Healthcare, Milwaukee, Wisconsin) with transmission and 32-channel receive head coils was used. Acquisition parameters for 3D TOF SPGR magnetic resonance angiography (MRA) were as follows: repetition time, 19 ms; bandwidth, 20.83 kHz; echo time, 4.3 ms; flip angle, 15 degrees; field of view (FOV), 12 × 12 cm^2; matrix size, 512 × 512; slice interval, 0.3 mm (after zero-fill interpolation [ZIP]); number of slices, 120; number of excitations [NEX], 2; no phase wrap; and acquisition time, 20 minutes 49 seconds. Imaging was first performed without contrast enhancement and then performed using contrast with 0.2 mL/kg gadodiamide hydrate (Omniscan; Daiichi-Sankyo, Tokyo, Japan).

This study was approved by the Ethics Committee at Iwate Medical University (H24-67). All subjects provided written informed consent.

Evaluation of the Labyrinthine Artery

Visibility of the labyrinthine artery was defined as at least 1 linear structure in the internal auditory canal depicted with and without contrast media (Omniscan), which appeared to be separated from the AICA. Visibility of the labyrinthine artery was evaluated by both authors (H.S. and K.K.) independently.

Data Analysis

To compare the detection rates of the labyrinthine artery between controls and patients with ISSHL, the χ^2 test was used. P values <.05 were considered significant.

Results

Magnetic resonance images of the labyrinthine artery are shown in **Figure 1**. The artery could be clearly seen in the anterior aspect of the internal auditory canal (left ear of a 30-year-old man, normal control; case 2). It was clearly detected both with and without contrast media. **Figure 2** shows another representative MRI of a normal control subject (case 3). In this noncontrast image, the labyrinthine artery could be depicted in both ears in the anterior aspect of the internal auditory canal. **Figure 3** shows an MRI of a patient with left ISSHL (25-year-old woman), which had been taken 18 days after onset. The labyrinthine artery could also be depicted in patients with ISSHL involving both ears, as in this case.

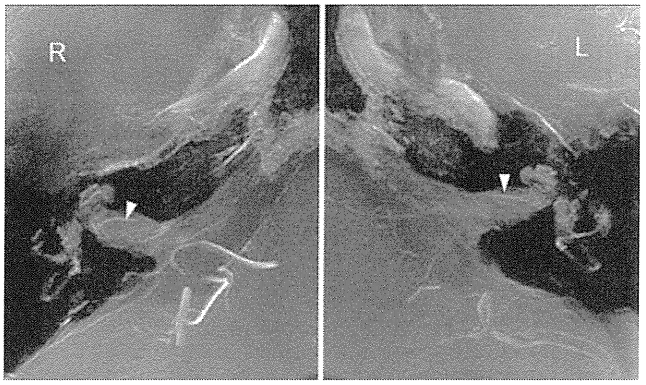

Figure 2. Representative magnetic resonance images of the labyrinthine artery in a normal control (right and left ear of a 33-year-old man, normal control; case 3). Images were taken without contrast (gadodiamide). The labyrinthine artery (arrowhead) can be clearly depicted in both ears as a linear structure in the internal auditory canal.

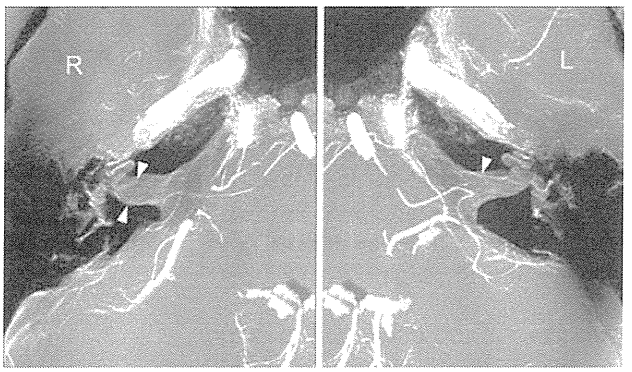

Figure 3. Magnetic resonance (MR) images of the labyrinthine artery in a patient with left idiopathic sudden sensorineural hearing loss (ISSHL) (25-year-old woman, ISSHL patient; case 1). These MR images were taken without contrast media 18 days after onset. Note that the labyrinthine artery can be clearly seen not only on the unaffected side (right, arrowhead) but also on the affected side (left, arrowhead).

Most of the subjects experienced transient dizziness when being moved into the gantry; however, no specific hazards were noted after the scanning. No subject was unable to be scanned due to the transient dizziness.

In 32 normal controls, the labyrinthine artery was depicted in 63 of 64 ears (98.4%). In 18 patients with ISSHL, it was detected in 36 of 36 ears (100%). There was no significant difference in detection rates between the 32 normal-hearing controls and the 18 patients with ISSHL (P = .769). Results of the visibility of the labyrinthine artery correlated well among authors. The locations of the labyrinthine arteries were mainly in the anterior aspect of the internal auditory canal. In 32 normal-hearing controls, it lay in the anterior aspect of the internal acoustic canal in 51 ears, in the middle aspect in 8 ears, and in the posterior aspect in 14 ears. Multiple positioned additional labyrinthine arteries (biarterial type) were observed in 8 of 64 ears. The labyrinthine artery lay in the anterior aspect in 32 of 36 ears in 18 patients with ISSHL, in the middle aspect in 5 ears, and in the posterior aspect in 3 ears. The biarterial type (**Figure 3**, right ear) was observed in 5 patients.

Demographic, audiologic, and MRI data from 18 patients with ISSHL are listed in **Table 2**. Intervals from onset of MRI examination varied from 3 to 54 days. As for hearing outcome, 8 patients showed complete recovery (CR), 9 patients had partial recovery (PR), and 1 patient had no recovery (NR). Hypertension, hyperlipidemia, and diabetes mellitus were observed in 4, 1, and 2 of the 18 patients with ISSHL, respectively. The labyrinthine artery was detected both with and without contrast media in all subjects.

Discussion

The labyrinthine artery usually arises from the apex of the loop of the AICA. It runs along the upper groove of the eighth cranial nerve toward the fundus of the internal acoustic meatus. In about 10% of individuals, it runs under the surface of the eighth cranial nerve in the internal acoustic meatus.[10] In the present study, most labyrinthine arteries were depicted in the anterior aspect of the internal auditory canal, the location of which coincides with the previous human temporal bone observations.[10]

Even a short period of ischemia can cause inner ear damage because the labyrinthine artery and its branches are end arteries with minimal collaterals from other major arterial branches.[11] With circulatory impairment of the AICA or the labyrinthine artery, cochlear symptoms, predominantly hearing loss, usually develop, and vertigo often occurs. Although it is rare, sudden hearing loss associated with vertigo in a patient with AICA occlusion without neurological deficits other than the eighth cranial nerve has been reported.[5] Kim et al[6] reported a patient who exhibited sudden hearing loss and vertigo, who then died 7 years later due to myocardial infarction. They found degeneration of the inner ear sensory epithelium as a result of reduced perfusion of the labyrinthine artery due to arteriosclerosis on postmortem examination. However, these reports lack direct evidence of vascular occlusion on imaging. To resolve this issue, visualization of the labyrinthine artery is absolutely necessary.

In the present study, 7-T MRI examinations with and without gadodiamide contrast were performed using the 3D TOF SPGR protocol. This ultra-high-field MRI unit enabled imaging of the labyrinthine artery, which until now has not been possible to depict. As a result, the depiction rate of the labyrinthine artery in the 32 normal-hearing controls was 98.4% (63 of 64 ears), and that in the 18 patients with ISSHL was 100% (36 of 36 ears). The detection rates and the magnetic resonance images obtained were basically the same both with and without contrast media. Therefore, contrast media is not necessary for the depiction of the labyrinthine artery. Extremely high depiction rates in the present study made it possible to evaluate the presence of a circulatory disturbance of the labyrinthine artery to some extent. To our knowledge, the present study is the first to report

Table 2. Demographic, audiologic, and MRI data of 18 patients with ISSHL.

			Hearing Level, dB				Depiction of LA		Cardiovascular RFs			
Patient No.	Age, y/Sex	Affected Ear	Initial, R/L	Final, R/L	Outcome	Days from Onset for MRI	Gd (–), R/L	Gd (+), R/L	HT	HL	DM	Alcohol Consumption
1	25/F	L	11/45	2/23	PR	18	+/+	+/+	–	–	–	No description
2	63/M	L	20/76	16/65	PR	10	+/+	+/+	+	–	–	1 drink/wk
3	25/F	R	106/14	70/14	PR	44	+/+	+/+	–	–	–	No description
4	36/F	R	103/ 4	59/ 2	PR	15	+/+	+/+	–	–	–	1–5 drinks/wk
5	56/F	R	111/12	72/11	PR	28	+/+	+/+	+	–	–	1 drink/wk
6	67/M	L	12/100	6/11	CR	14	+/+	+/+	–	–	–	>5 drinks/wk
7	34/M	L	10/75	2/11	CR	15	+/+	+/+	–	–	–	1–5 drinks/wk
8	65/F	L	21/111	16/77	PR	35	+/+	+/+	–	–	–	No description
9	25/M	R	48/19	17/13	CR	50	+/+	+/+	–	–	–	1–5 drinks/wk
10	64/M	R	110/22	56/21	PR	30	+/+	+/+	–	–	–	>5 drinks/wk
11	63/F	L	17/53	10/21	PR	21	+/+	+/+	–	–	–	1 drink/wk
12	64/F	L	19/55	20/30	CR	7	+/+	+/+	+	+	–	1 drink/wk
13	68/F	L	87/53	59/54	CR	23	+/+	+/+	–	–	–	1 drink/wk
14	75/M	L	28/74	29/74	NR	39	+/+	+/+	+	–	+	1–5 drinks/wk
15	62/F	R	71/11	15/13	CR	3	+/+	+/+	–	–	–	>5 drinks/wk
16	61/M	L	29/92	32/48	PR	7	+/+	+/+	–	–	–	>5 drinks/wk
17	64/M	L	26/80	23/21	CR	7	+/+	+/+	–	–	+	>5 drinks/wk
18	41/M	L	12/24	10/17	CR	54	+/+	+/+	–	–	–	1 drink/wk

Abbreviations: CR, complete recovery; Gd, gadodiamide; HT, hypertension; HL, hyperlipidemia; ISSHL, idiopathic sudden sensorineural hearing loss; L, left; LA, labyrinthine artery; DM, diabetes mellitus; MRI, magnetic resonance imaging; NR, no recovery; PR, partial recovery; R, right; RFs, risk factors.

depiction of the labyrinthine artery in humans using MRI. The labyrinthine artery could not be depicted in 1 ear of the normal-hearing controls. This was attributed to the variation in diameters of the labyrinthine artery. Its diameter has been reported to range from 200 to 900 μm[7] or from 68 to 140 μm.[8] Therefore, many can be depicted, but some are impossible to depict. In addition, one of the original 19 patients (5%) could not be evaluated due to motion artifact. This might be attributed to the length of acquisition time (20 minutes 49 seconds) rather than the strength of the magnetic field itself.

The labyrinthine artery could be depicted in all affected ears of 18 patients with ISSHL. These results seem to be quite natural because they showed some hearing recovery (8 complete recoveries and 9 partial recoveries) and, at the same time, they also suggest that occlusion of the labyrinthine artery is rare in the pathogenesis of ISSHL. The results obtained in the present study are compatible with the findings of temporal bone histopathology of patients with ISSHL; the hallmark of vascular insult to the cochlea, consisting of deposition of connective tissue and new bone, was observed in only 1 of 17 cases with ISSHL.[12]

Hypertension and diabetes mellitus were found in 22.2% (4 of 18 patients) and 11.1% (2 of 18 patients) of patients with ISSHL. In addition, 27.8% (5 of 18 patients) of patients with ISSHL consumed more than 5 alcoholic drinks per week. These cardiovascular risk factors were frequently seen in the present patients as reported by Lin et al.[1] However, an association between visibility of the labyrinthine artery and cardiovascular risk factors could not be observed.

The present study has a few limitations. First, the interval between the onset of hearing loss and the MRI examination ranged from 3 to 54 days. Thus, the magnetic resonance images obtained in this study do not reflect the images just after the onset of hearing loss. In other words, there remains the possibility that a transient ischemic event due to vasospasm could have been missed. Vasospasm might occur in the labyrinthine artery because it has a muscular media.[13,14] Second, other small arteries that supply the inner ear circulation, such as the common cochlear artery and the main cochlear artery, were not evaluated. Third, the sample size was small to conclude whether an inner ear circulatory disturbance is present in ISSHL. However, to our knowledge, no previous attempts to depict the labyrinthine artery have been reported. The present results have clinical significance in offering a useful method to evaluate circulatory disturbances of the labyrinthine artery.

Conclusion

The present study is the first to report depiction of the labyrinthine artery by 7-T MRI. The depiction rate of the labyrinthine artery was 98.4% (63 of 64 ears) in 32 normal-hearing controls and 100% (36 of 36 ears) in 18 patients with ISSHL. These preliminary results indicate that occlusion of the labyrinthine artery would be rare in the pathogenesis of

ISSHL, and they also demonstrate that the labyrinthine artery could be detected by ultra-high-field MRI.

Acknowledgment

We thank Makoto Sasaki, MD, PhD, Chair, Core of Multidisciplinary Research for Medical Imaging, Professor, Section for Ultrahigh-Field MRI, for his helpful technical advice and support during the preparation of this research.

Author Contributions

Hiroaki Sato, conception and design, main revision of the manuscript; **Kazuaki Kawagishi**, acquisition of data, analysis.

Disclosures

Competing interests: None.

Sponsorships: None.

Funding source: Grant-in-aid for the Strategic Medical Science Research Center from the Ministry of Education, Culture, Sport, Science, and Technology and a grant from the Ministry of Health, Labor and Welfare of Japan.

References

1. Lin RJ, Krall R, Westerberg BD, Chadha NK, Chau JK. Systematic review and meta-analysis of the risk factors for sudden sensorineural hearing loss in adults. *Laryngoscope*. 2012;122:624-635.
2. Hinojosa R, Kohut RI. Clinical diagnosis of anterior inferior cerebellar thrombosis: autopsy and temporal bone histopathology study. *Ann Otol Rhinol Laryngol*. 1990;90:261-271.
3. Oas JG, Baloh RW. Vertigo and the anterior inferior cerebellar artery syndrome. *Neurology*. 1992;42:2274-2279.
4. Lee H, Sohn SI, Jung DK, et al. Sudden deafness and anterior inferior cerebellar artery infarction. *Stroke*. 2002;33:2807-2812.
5. Lee H, Ahn BH, Baloh RW. Sudden deafness with vertigo as a sole manifestation of anterior inferior cerebellar artery infarction. *J Neural Sci*. 2004;222:105-107.
6. Kim JS, Lopez I, DiParte PL, Liu F, Ishiyama A, Baloh RW. Internal auditory artery infarction: clinicopathologic correlation. *Neurology*. 1999;52:40-44.
7. Levin NA. The vascularization of the ear labyrinth in man [in German]. *Anat Anz*. 1964;114:337-352.
8. Ishii T. Arteries from basal brain to inner ear: observation of 20 Japanese [in Japanese]. *Nihon Jibiinkoka Gakkaiho*. 1964; 67:1387-1399.
9. Stachler RJ, Chandrasekhar SS, Archer SM, et al. Clinical practice guideline: sudden hearing loss. *Otolaryngol Head Neck Surg*. 2012;146(suppl):S1-S35.
10. Mazzoni A. Internal auditory canal arterial relations at the porus acousticus. *Ann Otol Rhinol Laryngol*. 1969;78:797-814.
11. Perlman HB, Kimura RS, Fernandez C. Experiments on temporary obstruction of the internal auditory artery. *Laryngoscope*. 1959;69:591-613.
12. Merchant SN, Adams JC, Nadol JB. Pathology and pathophysiology of idiopathic sudden sensorineural hearing loss. *Otol Neurotol*. 2005;26:151-160.
13. Axelsson A, Ryan AF. Circulation of the inner ear, I: comparative study of the vascular anatomy in the mammalian cochlea. In: Jahn AF, Santos-Sacchi J, eds. *Physiology of the Ear*. New York, NY: Raven; 1988:295-315.
14. Mom T, Telischi FF, Martin GK, Stagner BB, Lonsbury-Martin BL. Vasospasm of the internal auditory artery: significance in cerebellopontine-angle surgery. *Am J Otol*. 2000;21:735-742.

Hearing Research 302 (2013) 26–31

Contents lists available at SciVerse ScienceDirect

Hearing Research

journal homepage: www.elsevier.com/locate/heares

Research paper

RNA analysis of inner ear cells from formalin fixed paraffin embedded (FFPE) archival human temporal bone section using laser microdissection – A technical report

Yurika Kimura [a,b,*], Sachiho Kubo [b], Hiroko Koda [c,d], Kazuhiro Shigemoto [b], Motoji Sawabe [e], Ken Kitamura [c]

[a] Department of Otolaryngology, Tokyo Metropolitan Geriatric Medical Hospital, 35-2, Sakae-cho, Itabashi, Tokyo 173 0015, Japan
[b] Research Team for Geriatric Medicine, Tokyo Metropolitan Institute of Gerontology, Sakae-cho, Itabashi, Tokyo, Japan
[c] Department of Otolaryngology, Graduate School, Tokyo Medical and Dental University, Yushima, Bunkyo, Tokyo, Japan
[d] Department of Otolaryngology, Ohkubo Hospital, Kabukicho, Shinjuku, Tokyo, Japan
[e] Section of Molecular Pathology, Graduate School of Health Care Sciences, Tokyo Medical and Dental University, Japan

ARTICLE INFO

Article history:
Received 1 January 2013
Received in revised form
16 April 2013
Accepted 22 April 2013
Available online 6 May 2013

ABSTRACT

Objective: Molecular analysis using archival human inner ear specimens is challenging because of the anatomical complexity, long-term fixation, and decalcification. However, this method may provide great benefit for elucidation of otological diseases. Here, we extracted mRNA for RT-PCR from tissues dissected from archival FFPE human inner ears by laser microdissection.

Methods: Three human temporal bones obtained at autopsy were fixed in formalin, decalcified by EDTA, and embedded in paraffin. The samples were isolated into spiral ligaments, outer hair cells, spiral ganglion cells, and stria vascularis by laser microdissection. RNA was extracted and heat-treated in 10 mM citrate buffer to remove the formalin-derived modification. To identify the sites where *COCH* and *SLC26A5* mRNA were expressed, semi-nested RT-PCR was performed. We also examined how long *COCH* mRNA could be amplified by semi-nested RT-PCR in archival temporal bone.

Results: COCH was expressed in the spiral ligament and stria vascularis. However, *SLC26A5* was expressed only in outer hair cells. The maximum base length of *COCH* mRNA amplified by RT-PCR was 98 bp in 1 case and 123 bp in 2 cases.

Conclusion: We detected *COCH* and *SLC26A5* mRNA in specific structures and cells of the inner ear from archival human temporal bone. Our innovative method using laser microdissection and semi-nested RT-PCR should advance future RNA study of human inner ear diseases.

1. Introduction

Mechanisms of sensorineural hearing loss have been analysed using advanced molecular techniques. Molecular genetic studies of experimental animals including mice have identified genes involved in deafness and have determined genotype–phenotype correlations (Gibson et al., 1995, Everett et al., 2001). However, molecular analysis using fixed and embedded human inner ear specimens has been challenging because they are usually inaccessible. While formalin-fixation and celloidin-embedding are standard histopathological methods for human temporal bone specimens, they are unsuitable for molecular analysis (Schuknecht, 1993). However, there are several reports in which DNA has been successfully extracted and analysed from human inner ear specimens. Genes involved in deafness were identified using a cDNA library from the human fetal inner ear (Robertson et al., 1998), and quantitative analysis of a mitochondrial DNA (mtDNA) mutation using archival temporal bones was reported (Takahashi et al., 2003, Koda et al., 2010). Recently, mitochondrial DNA deletions were

Abbreviations: FFPE, formalin fixed paraffin embedded; EDTA, ethylenediaminetetraacetic acid; mtDNA, mitochondrial DNA; LMD, laser microdissection; SV, stria vascularis; SGC, spiral ganglion cells; OHC, outer hair cells; SL, spiral ligament.

* Corresponding author. Department of Otolaryngology, Tokyo Metropolitan Geriatric Medical Hospital, 35-2, Sakae-cho, Itabashi, Tokyo 173 0015, Japan. Tel.: +81 3 3964 1141; fax: +81 3 3964 1982.
E-mail address: kimura@tmghig.jp (Y. Kimura).

0378-5955/$ – see front matter © 2013 Elsevier B.V. All rights reserved.
http://dx.doi.org/10.1016/j.heares.2013.04.008

detected in human inner ears from patients with presbycusis by laser microdissection (Markaryan et al., 2009).

In contrast to DNA analysis, RNA expression analysis can demonstrate the spatio-temporal activities of gene transcription and expression in tissues, providing important physiological and pathological information. Further, mRNA analysis is important because it examines the "working copy" of a gene. Therefore, studying mRNA extracted from human inner ears can provide further information concerning the molecular mechanisms of inner ear disorders of humans. Previously, we established an optimal method of extracting mRNA suitable for molecular biological applications from the autopsy specimens of human temporal bones (Kimura et al., 2007). However, this method uses frozen whole cochlea, and can not be applied to the retrospective analyses using formalin-fixed archival temporal bone specimens.

The objective of this study was to establish an optimal method of RNA expression analysis of specific sites in the human inner ear using archival (stored) FFPE human inner ear specimens and the laser microdissection techniques.

2. Materials and methods

2.1. Temporal bones

Three human temporal bones from individuals with no hearing impairment according to nursing records were obtained at autopsy. The cases were 2 males and 1 female of 70, 71, and 71 years of age, respectively. The post-mortem time before autopsy ranged from 1 to 15 h. The temporal bones were fixed in buffered 20% formalin at room temperature for 12–20 months, followed by decalcification in 10% ethylenediaminetetraacetic acid (EDTA) for 6–9 months at room temperature. After decalcification, the specimens, including the bony labyrinth, was cropped to a cube measuring 15 mm to fit standard plastic cassettes and glass slides. The specimens were embedded in paraffin, serially cut into 6 μm-thick thin sections, and mounted on a membrane slide for laser microdissection.

2.2. Laser microdissection

After deparaffinization of the thin sections by xylene and staining with toluidine blue, the spiral ligaments, spiral ganglion cells, stria vascularis, and outer hair cells in the basal turn were isolated using a laser microdissection system (Leica AS LMD; Wetzlar, Germany). This system uses a UV laser to isolate microscopic regions from samples. Tissue fragments from 3 successive sections of inner ear were placed gently into 0.5 ml microtubes filled with 50 μl tissue lysis buffer. The specimens were not touched, which makes specimen collection by gravity a contamination-free procedure.

2.3. RNA extraction

RNA extraction and cDNA synthesis was performed using the methods described by Hamatani et al. (2006). RNA was isolated from the microdissected tissue using the High Pure RNA Paraffin Kit (Roche Diagnostics; Basel, Switzerland) according to the manufacturer's protocols with some modifications. Briefly, microdissected tissue was digested with proteinase K at 55 °C overnight, followed by DNase I treatment. After the lysate was purified by the High Pure filter, RNA was eluted twice with 100 μl of RNase-free water. RNA was then precipitated by ethanol in the presence of 2 μl of ethachinmate (Nippon Gene; Tokyo, Japan), which is a carrier solution for the alcohol precipitation of DNA and RNA and resuspended in 30 μl of RNase-free water. The concentration of RNA was measured by absorption at 260 nm with GeneQuant 1300 (GE Healthcare UK Ltd; Buckinghamshire, England).

2.4. Heat treatment of RNA

Approximately 150 ng of total RNA was heated in 250 μl of 10 mM citrate buffer pH 4.0 at 70 °C for 45 min. After 25 μl sodium acetate was added into the solution, RNA was precipitated by ethanol in the presence of ethachinmate as a carrier, dried, and dissolved in RNase-free water to the final concentration of 10 ng/μl.

2.5. cDNA synthesis

The 11 μl of RNase-free solution containing 90 ng of total RNA and 50 pmol/ml of random primers was heated at 65 °C for 10 min and chilled in ice water. A mixture consisting of 4 μl of 5 × RT buffer, 2 μl of 20 mM DTT, 1 μl of 10 mM dNTPs, 1 μl of RNase Inhibitor (10 U/μl), and 1 μl of ReverTra Ace (Toyobo, Osaka, Japan) was added to the RNA solution and incubated at 42 °C for 60 min and at 70 °C for 15 min.

2.6. RT-PCR of COCH and SLC26A5 mRNA

We selected *COCH* and *SLC26A5* as the target genes for RT-PCR because cochlin, coded by *COCH* (accession No. NM_001135058), is the protein expressed most commonly in the inner ear other than collagen, and prestin, coded by *SLC26A5* (accession No. NG_023055) is a motor protein expressed specifically in outer hair cells. *GAPDH* (accession No.NG_007073), a typical house-keeping gene, was used for standardization. In order to detect very small amounts of target cDNA and to reduce the contamination in products due to the amplification of unexpected primer binding sites, semi-nested RT-PCR was performed. Forward and reverse primers were designed to cover different exons and introns to prevent a carry-on of the genomic DNA, in order not to detect a carry-on of genomic DNA using the free program on the internet, Primer 3 (http://primer3.sourceforge.net/). Primer sequences are shown in Table 1.

First RT-PCR was performed in a 20 μl volume containing 10 μl Premix Taq® (Takara Bio, Otsu, Japan), 0.5 μM of each specific primer and 1 μl of cDNA from the RT reaction. After an initial incubation at 94 °C for 3 min, the reaction mixtures were subjected to 30 cycles of amplification using the following sequence: 94 °C for 30 s, 55 °C for 30 s, and 72 °C for 45 s. This was followed by a final extension step at 72 °C for 7 min. The second RT-PCR was carried out in a 20 μl mixture containing 10 μl Premix Taq®, 0.5 μM of each specific primer and 1 μl of 9× first RT-PCR product following the same sequence of the first RT-PCR. Finally, 8 μl of the reaction mixture was run on a 3% agarose gel and visualized with ethidium bromide.

2.7. RT-PCR of COCH with different sizes of PCR products

To elucidate how long mRNA could be preserved in very small samples microdissected from formalin-fixed, long-term EDTA-decalcified, and paraffin-embedded thin sections, cDNA of *COCH* from the specimens of the spiral ligament was amplified using 5 sets of primers that would yield PCR products of different sizes from 98 to 180 bp as shown in Tables 2 and 3, and Fig. 1, with the second PCR product size of 87 bp.

Table 1
Primer sequences and product sizes for semi-nested RT-PCR of *COCH*, *SLC26A5*, and *GAPDH* mRNA.

mRNA	Forward primer	Reverse primer for the first PCR	Reverse primer for the second PCR	Product size of the first PCR	Product size of the second PCR
COCH	GGCATCCAGTCTCAAATGCT	GTGCTGTGGACACTGCTTGT	GTCCTGTGGCCTCCTGTGTA	103	85
SLC26A5	GTCTCGAAGCCTTGTTCAGG	GGGCAATGATTCAAAGAGGA	GGAAGACACAGCTTGCAGGT	118	86
GAPDH	AATGACCCCTTCATTGACCTC	ATGGGATTTCCATTGATGACA	TTCCATTGATGACAAGCTTCC	122	115

2.8. Ethical considerations

Consent for using temporal bone tissues removed at autopsy was obtained from the patients' relatives. The present study was approved by the Ethical Review Board at Tokyo Metropolitan Geriatric Medical Hospital, pursuant to Article 18 of the Cadaver Autopsy and Preservation Act.

3. Results

3.1. Laser microdissection

The microdissected areas in the cochlea are shown in Fig. 2. The outer hair cells, spiral ganglion cells, the stria vascularis, and the spiral ligament were dissected separately.

3.2. Site-specific expression of COCH and SLC26A5 in the cochlea

The results of *COCH* and *SLC26A5* site-specific expression are shown in Figs. 3 and 4. *COCH* expression was detected only in the spiral ligament and the stria vascularis, and *SCL26A5* was expressed in the outer hair cells only. *GAPDH* expression was detected in all of the structures examined.

3.3. RT-PCR of COCH with different sizes of PCR products

The maximum length of PCR amplicons for the first RT-PCR was 98 bp in 1 case and was 123 bp in 2 cases in each experiment (Fig. 5). These results suggest that approximately 100 bp was the maximum preserved length of mRNA after the long-term successive processing of formalin fixation, EDTA decalcification, and paraffin embedding.

Table 2
Primer sequences for semi-nested RT-PCR of *COCH* mRNA.

	Primer codes	Primer sequences
Forward primer	F	CAC ATG TGG GCC TTG TTC AA
Reverse primer	R1	CAA ACA AAA CAT CTT TGG CTG A
	R2	TTC CTT TAT GGC AAA CAA AAC A
	R3	TGG AAT TAC CCC CTC TGA AA
	R4	TGC TTC AAG GCT TTT CCT GT
	R5	CCG TGA AGA ATT TCT GAG CA
	R6	CTC CAG CAT CTA CCG TGA AG

Table 3
The product sizes of semi-nested RT-PCR of *COCH* mRNA.

Primer combination of first PCR	Product size of first PCR (bp)	Primer combination of second PCR	Product size of second PCR (bp)
F-R2	98	F-R1	87
F-R3	123		
F-R4	145		
F-R5	168		
F-R6	180		

The primer codes are defined in Table 2.

4. Discussion

We have successfully optimized a semi-nested RT-PCR method of detecting *COCH* and *SLC25A5* expression from specific sites of the inner ear using archival FFPE human inner ear specimens and the laser microdissection techniques. The maximal size of the *COCH* PCR amplicons was 98 bp and 123 bp.

4.1. DNA study of inner ears

Wackym et al. reported the first molecular analysis of human temporal bone pathology in 1993 (Wackym et al., 1993). However, DNA analysis of the whole section, as in their method, is of limited value because the inner ear is composed of heterogeneous and highly differentiated cells. Laser microdissection is a useful tool that allows the combination of morphological analysis and molecular biological analysis. We introduced this method for mitochondrial DNA analysis in the human temporal bone for the first time (Kimura et al., 2005), and elucidated a correlation between the mtDNA mutation rate and atrophy of the stria vascularis, as well as decreases in spiral ganglion cells (Koda et al., 2010). Markaryan et al. reported a large scale deletion of mtDNA in the cochlea and showed that major arc mtDNA deletions contributed to the observed deficit in *COX3* expression (Markaryan et al., 2009). These results suggest a correlation between presbycusis and the deletion of mtDNA in the cochlea.

4.2. mRNA expression study of the inner ear

Although DNA analysis using the laser microdissection method has become established to some degree, gene expression analysis of targeted mRNA remains challenging because RNA is more susceptible to strand breakage and cross linking by formalin fixation than DNA after fixation and decalcification (Chung and Hewitt, 2010). To overcome this difficulty, several research groups have attempted RNA analysis of archival human temporal bones. Lee et al. reported the first study of RT-PCR for archival temporal bones in 1997, in which they examined the expression of the γ-actin gene (Lee et al., 1997). In their report, the expression of γ-actin mRNA was detected in only one of ten archival temporal bone specimens, and the authors concluded that the analysis of gene expression from an archival section was very limited because the mRNA had been degraded by RNases. Lin et al. reported the RNA analysis of temporal bone soft tissues (Lin et al., 1999). They harvested temporal bones at immediate autopsies and showed the manifestations and

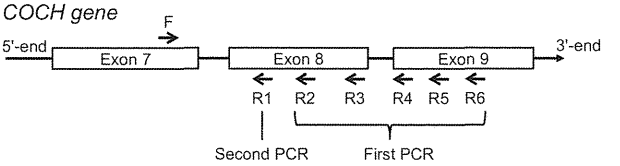

Fig. 1. Positions of forward and reverse primers that were used to elucidate the maximum preserved size of mRNA in the *COCH* gene. Forward and reverse primers were designed to cover different exons and introns and not to detect a carry-on of genomic DNA.

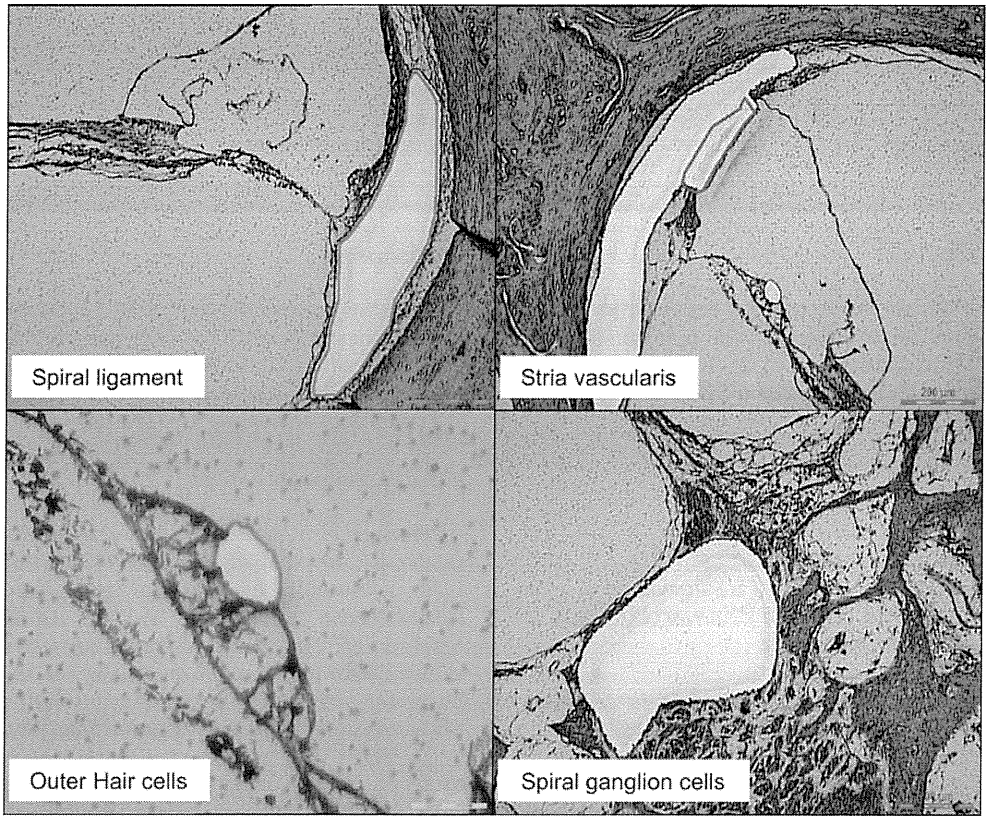

Fig. 2. Histological images of the spiral ligament, spiral ganglion cells, the stria vascularis and outer hair cells in the basal turn of the inner ear. After deparaffinization of the thin sections by xylene and staining with toluidine blue, the spiral ligaments, spiral ganglion cells, stria vascularis, and outer hair cells in the basal turn were isolated using a laser microdissection system (Leica AS LMD; Wetzlar, Germany). All microdissected tissue fragments from 3 successive tissue sections were collected into 0.5 ml microtubes filled with 50 μl tissue lysis buffer.

localizations of mRNA of mucin genes, such as *MUC5B* and *MUC1*, in the submucosal gland of the Eustachian tube and the middle ear. They suggested a high possibility of RNA analysis within 6 h of death. Under clinical circumstances, however, it is not realistic to harvest a temporal bone in 6 h after death. We developed a method of detection of *COCH* mRNA expression, as well as *GAPDH* mRNA expression using RNA extracted from membranous labyrinths dissected from formalin-fixed or frozen human cochlea (Kimura et al., 2007). This method is useful because removal of temporal bone specimens could be incorporated into the protocol of a conventional autopsy. However, this method was not able to utilize archival sections effectively. Hall et al. reported optimization of RNA detection from archival guinea pig temporal bones by the Trizol extraction method (Hall et al., 2007). This approach may be useful,

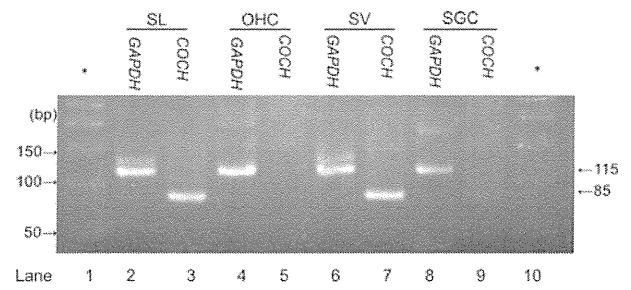

Fig. 3. Optimized semi-nested RT-PCR analysis of *GAPDH* and *COCH* in the FFPE human cochlea. The length of amplicons of *GAPDH* and *COCH* is 85 bp and 115 bp. Lane 1 and 10 are 50 bp ladder markers (asterisks(*)). Lane 2 and 3, semi-nested RT-PCR results from the spiral ligament(SL) using primers to GAPDH and COCH. Lane 4 and 5, semi-nested RT-PCR results from outer hair cells (OHC) using primers to GAPDH and COCH. Lane 6 and 7, semi-nested RT-PCR results from the stria vascularis (SV) using primers to GAPDH and COCH. Lane 8 and 9, semi-nested RT-PCR results from the spiral ganglion cells (SGC) using primers to GAPDH and COCH. Universal expression of *GAPDH* is noted. *COCH* is expressed in the spiral ligament and the stria vascularis, but is not expressed in the outer hair cells and spiral ganglion cells.

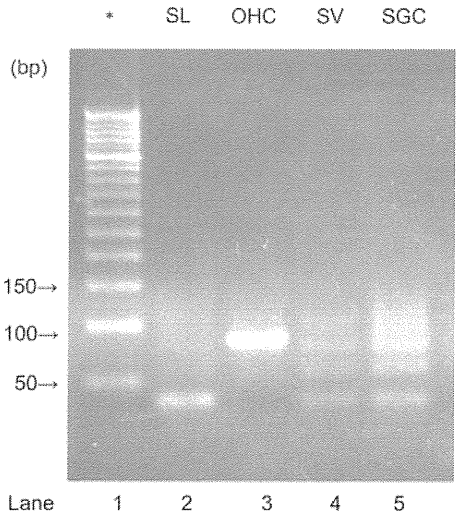

Fig. 4. Optimized semi-nested RT-PCR analysis of *SLC26A5* in the FFPE human cochlea. The length of the amplicon of *SLC26A5* is 86 bp. Lane 1 is 50 bp ladder markers (an asterisk(*)). Lane 2 to 5, semi-nested RT-PCR results from the spiral ligament(SL), the outer hair cells (OHC), the stria vascularis (SV) and spiral ganglion cells (SGC) using primers to *SLC26A5*. *SLC26A5* is expressed in the outer hair cells, but is not expressed in the spiral ligament, the stria vascularis, and the spiral ganglion cells.

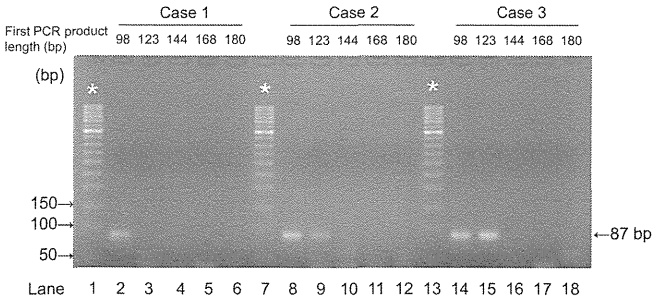

Fig. 5. Optimized semi-nested RT-PCR analysis of *COCH* to elucidate the maximum preserved length of mRNA extracted from FFPE human cochlea by using different reverse primers in first RT-PCR. Lane 1, 7 and 13 are 50 bp ladder markers (asterisks(*)). Lane 2 to 6, semi nested RT-PCR of *COCH* of the stria vascularis of case 1. Lane 8 to 12, semi nested RT-PCR of *COCH* of the stria vascularis of case 2. Lane 14 to 18, semi nested RT-PCR of *COCH* of the stria vascularis of case 3. Lane 2, 8 and 14 are the semi nested RT-PCR products of which first RT-PCR product length is 98 bp. Lane 3, 9 and 15 are the semi nested RT-PCR products of which first RT-PCR product length is 123 bp. Lane 4, 10 and 16 is the semi nested RT-PCR product of which first RT-PCR product length is 144 bp. Lane 5, 11 and 17 are the semi nested RT-PCR products of which first RT-PCR product length is 168 bp. Lane 6, 12 and 18 are the semi nested RT-PCR products of which first RT-PCR product length is 180 bp. The length of semi-nested PCR products is 87 bp. Up to 123 bp can be preserved in two cases and up to 98 bp in one case.

but it is not clear that this method could be applied to human archival inner ear specimens dissected by laser microdissection because, in their study, whole sections of the temporal bone were used and the period of fixation and decalcification was much shorter than those used for human samples.

4.3. mRNA expression study using tiny tissue samples that were laser-microdissected from archival human FFPE temporal bone

Pagedar et al. were the first to succeed in the analysis of RNA of the human inner ear from FFPE tissue using laser capture microdissection (Pagedar et al., 2006). They examined the vestibular organ dissected from a temporal bone block before fixation, and not archival cochlea samples. Therefore, our trial to extract mRNA from laser microdissected tissue (outer hair cells, the stria vascularis, spiral ganglion cells, and the spiral ligament) of human archival FFPE temporal bone sections was extremely challenging. Hamatani et al. indicated that RT-PCR amplification of degraded RNA extracted from archival unbuffered formalin-fixed, paraffin-embedded thyroid cancer tissue samples, which were preserved at room temperature for 19–21 years, could be improved by heating RNA in citrate buffer prior to cDNA synthesis (Hamatani et al., 2006). Since FFPE-derived RNA is degenerated into very short fragments and chemically modified, and reverse transcription from polyA tail is inefficient, the use of random primers instead of Oligo dT primers was recommended for cDNA synthesis (Farragher et al., 2008). Using these ideas and semi-nested PCR enabled us to amplify extremely small amounts of nucleic acid, and to extract mRNA from laser microdissected tissue of human archival FFPE temporal bone sections. Hamatani et al. reported that longer fragments up to 250 bp in the preheated RNA could be amplified in all cases compared with the non-treated RNA (Hamatani et al., 2006), while only very short fragments of RNA of approximately 100 bp could be obtained in our study. The fragmentation of the RNA strands could be ascribed to different tested organs (temporal bone in our study vs. thyroid tissue in their study), longer formalin fixation-period, and long-term decalcification in our study. These disadvantages, such as a long-period of formalin fixation and decalcification, influence the preservation of morphology such as shrinkage of tissue. Takahashi et al. reported excellent immunostaining results for the human cochlea, such as immunostaining for prestin in the cytoplasm of the human outer hair cells (Takahashi et al., 2010). We consider that the complementary use of molecular and immunohistochemical techniques will become a valuable tool for future study of the human inner ear.

5. Conclusions

Although molecular analysis using human inner ear specimens is challenging because of the anatomical complexity and long-term fixation and decalcification, it can provide significant data for the elucidation of otological disorders. We extracted mRNA from archival FFPE human inner ears by laser microdissection, and detected site-specific *COCH and SLC26A5* mRNA expression by RT-PCR from archival human temporal bones. We hope our innovative methods will pave the way for future RNA analyses of human inner ear disease.

Acknowledgements

This study was supported by Grants-in-Aid for Scientific Research (Nos. 19791250, 21390459, 22659305, 23791953) from the Ministry of Education, Culture, Sports, Science and Technology, Japan. The authors wish to thank Mr Goto, Mr Mukaiyama, Ms Hasegawa, and all other technicians in the Departments of Pathology of Tokyo Metropolitan Geriatric Hospital for their excellent pathological work. We also express our sincere gratitude to the deceased whose temporal bones contributed to this study.

References

Chung, J.Y., Hewitt, S.M., 2010. An optimized RNA extraction method from archival formalin-fixed paraffin-embedded tissue. Methods Mol. Biol. 611, 19–27.
Everett, L.A., Belyantseva, I.A., Noben-Trauth, K., Cantos, R., Chen, A., Thakkar, S.I., Hoogstraten-Miller, S.L., Kachar, B., Wu, D.K., Green, E.D., 2001. Targeted disruption of mouse Pds provides insight about the inner-ear defects encountered in Pendred syndrome. Hum. Mol. Genet. 10, 153–161.
Farragher, S.M., Tanney, A., Kennedy, R.D., Harkin, P.D., 2008. RNA expression analysis from formalin fixed paraffin embedded tissues. Histochem. Cell. Biol. 130, 435–445.
Gibson, F., Walsh, J., Mburu, P., Varela, A., Brown, K.A., Antonio, M., Beisel, K.W., Steel, K.P., Brown, S.D., 1995. A type VII myosin encoded by the mouse deafness gene shaker-1. Nature 374, 62–64.
Hall, K.L., Pitts, D.R., Anne, S., Semaan, M.T., Alagramam, K.N., Megerian, C.A., 2007. Optimization of ribonucleic acid detection from archival Guinea pig temporal bone specimens. Otol Neurotol. 28, 116–123.
Hamatani, K., Eguchi, H., Takahashi, K., Koyama, K., Mukai, M., Ito, R., Taga, M., Yasui, W., Nakachi, K., 2006. Improved RT-PCR amplification for molecular analyses with long-term preserved formalin-fixed, paraffin-embedded tissue specimens. J. Histochem. Cytochem. 54 (7), 773–780.
Kimura, Y., Kouda, H., Kobayashi, D., Suzuki, Y., Ishige, I., Iino, Y., Kitamura, K., 2005. Detection of mitochondrial DNA from human inner ear using real-time polymerase chain reaction and laser microdissection. Acta Otolaryngol. 125, 697–701.
Kimura, Y., Kubo, S., Koda, H., Noguchi, Y., Sawabe, M., Maruyama, N., Kitamura, K., 2007. Quantitative analysis of mRNA in human temporal bones. Acta Otolaryngol. 127 (10), 1024–1030.
Koda, H., Kimura, Y., Ishige, I., Eishi, Y., Iino, Y., Kitamura, K., 2010. Quantitative cellular level analysis of mitochondrial DNA 3243A>G mutations in individual tissues from the archival temporal bones of a MELAS patient. Acta Otolaryngol. 130 (3), 344–350.
Lee, K.H., McKenna, M.J., Sewell, W.F., Ung, F., 1997. Ribonucleases may limit recovery of ribonucleic acids from archival human temporal bones. Laryngoscope 107, 1228–1234.
Lin, J., Kawano, H., Paparella, M.M., Ho, S.B., 1999. Improved RNA analysis for immediate autopsy of temporal bone soft tissues. Acta Otolaryngol. 119, 787–795.
Markaryan, A., Nelson, E.G., Hinojosa, R., 2009. Quantification of the mitochondrial DNA common deletion in presbycusis. Laryngoscope 119, 1184–1189.
Pagedar, N.A., Wang, W., Chen, D.H., Davis, R.R., Lopez, I., Wright, C.G., Alagramam, K.N., 2006. Gene expression analysis of distinct populations of cells isolated from mouse and human inner ear FFPE tissue using laser capture microdissection–a technical report based on preliminary findings. Brain Res. 1091 (1), 289–299.
Robertson, N.G., Lu, L., Heller, S., Merchant, S.N., Eavey, R.D., McKenna, M., Nadol Jr., J.B., Miyamoto, R.T., Linthicum Jr., F.H., Lubianca Neto, J.F., Hudspeth, A.J., Seidman, C.E., Morton, C.C., Seidman, J.G., 1998. Mutations in a

novel cochlear gene cause DFNA9, a human nonsyndromic deafness with vestibular dysfunction. Nat. Genet. 20, 299–303.
Schuknecht, H., 1993. Pathology of the Ear, second ed. Lea & Febiger, Philadelphia.
Takahashi, K., Merchant, S.N., Miyazawa, T., Yamaguchi, T., McKenna, M.J., Kouda, H., Iino, Y., Someya, T., Tamagawa, Y., Takiyama, Y., Nakano, I., Saito, K., Boyer, P., Kitamura, K., 2003. Temporal bone histopathological and quantitative analysis of mitochondrial DNA in MELAS. Laryngoscope 113, 1362–1368.
Takahashi, M., Kimura, Y., Sawabe, M., Kitamura, K., 2010. Modified paraffin-embedding method for the human cochlea that reveals a fine morphology and excellent immunostaining results. Acta Otolaryngol. 130, 788–792.
Wackym, P.A., Simpson, T.A., Gantz, B.J., Smith, R.J., 1993. Polymerase chain reaction amplification of DNA from archival celloidin-embedded human temporal bone sections. Laryngoscope 103, 583–589.

Neuroscience Letters 561 (2014) 91–95

Contents lists available at ScienceDirect

Neuroscience Letters

journal homepage: www.elsevier.com/locate/neulet

The influence of sphingosine-1-phosphate receptor antagonists on gentamicin-induced hair cell loss of the rat cochlea

Masahiro Nakayama, Keiji Tabuchi*, Tomofumi Hoshino, Mariko Nakamagoe, Bungo Nishimura, Akira Hara

Department of Otolaryngology, Faculty of Medicine, University of Tsukuba, Tsukuba, Japan

HIGHLIGHTS

- Sphingosine-1-phosphate (S1P) receptors 1–3 ($S1PR_{1-3}$) were expressed in the organ of Corti and spiral ganglion.
- An $S1PR_2$ antagonist increased gentamicin-induced hair cell loss.
- These results indicate a possibility that S1P act as a cochlear protectant against gentamicin ototoxicity via activation of $S1PR_2$.

ARTICLE INFO

Article history:
Received 30 October 2013
Received in revised form
20 December 2013
Accepted 27 December 2013

Keywords:
Sphingosine-1-phosphate (S1P)
S1P receptor (S1PR)
Gentamicin ototoxicity
Cochlea hair cell loss

ABSTRACT

Sphingosine-1-phosphate (S1P) is a sphingolipid metabolite that regulates various critical biological processes, such as cell proliferation, survival, migration, and angiogenesis. The action of S1P is exerted by its binding to 5 specific G protein-coupled S1P receptors (S1PR), $S1PR_1$–$S1PR_5$. Aminoglycoside antibiotics including gentamicin induce cochlear hair cell loss and sensorineural hearing loss. Apoptotic cell death is considered to play a key role in this type of cochlear injury. S1P acts as a cochlear protectant against gentamicin ototoxicity. In the present study, expression of S1PRs in the cochlea was examined. In addition, the effects of S1PR antagonists on gentamicin ototoxicity were investigated using tissue culture techniques. Cochleas were dissected from Sprague-Dawley rats on postnatal days 3–5. Basal turn organ of Corti explants were exposed to 35 μM gentamicin for 48 h with or without S1PR antagonists. $S1PR_{1-3}$ were expressed in the organ of Corti and spiral ganglion. The $S1PR_2$ antagonist increased gentamicin-induced hair cell loss, while the $S1PR_1$ and $S1PR_3$ antagonists did not affect gentamicin ototoxicity. These results indicate the possibility that S1P act as a cochlear protectant against gentamicin ototoxicity via activation of $S1PR_2$.

1. Introduction

Sphingolipid metabolites, such as ceramides and sphingoid bases, have been implicated in the modulation of membrane signal transduction systems and in diverse cellular processes, such as cell proliferation, survival, migration, and angiogenesis [1–4]. We recently reported that exogenously applied sphingosine-1-phosphate (S1P) protected cochlear hair cells against gentamicin ototoxicity [5]. S1P exerts its cellular responses through a family of 5 G-protein-coupled S1P receptors (S1PRs) known as $S1PR_{1-5}$ [6–9]. These S1PRs are differentially expressed in various cell types. $S1PR_1$, $S1PR_2$, and $S1PR_3$ are widely expressed in cells and tissues, whereas $S1PR_4$ and $S1PR_5$ are expressed only in the cells of the immune and nervous systems [10]. Presence of $S1PR_{1-3}$ has been shown in the organ of Corti [11,12], but expression of $S1PR_{4,5}$ has never been examined before.

Aminoglycoside antibiotics are widely used for the treatment of infectious diseases. However, the clinical usage of aminoglycosides has often been limited owing to their side effects – ototoxicity and nepherotoxicity. Aminoglycosides are well known to damage cochlear inner ear hair cells, causing sensorineural hearing loss and balance disturbance [12]. Recent findings have demonstrated that death of cochlear hair cells was elicited by gentamicin via an apoptotic pathway, at least in part [13,14]. Particularly, evidence of the involvement of the intrinsic apoptotic pathway in gentamicin ototoxicity has been demonstrated [15].

The present study was designed to investigate the expression of S1PRs in the rat cochlea and to examine the role of S1PRs in hair cell death induced by gentamicin.

* Corresponding author at: Department of Otolaryngology, Faculty of Medicine, University of Tsukuba, 1-1-1 Tennodai, Tsukuba 305-8575, Japan.
Tel.: +81 298 53 3147; fax: +81 298 53 3147.
E-mail address: ktabuchi@md.tsukuba.ac.jp (K. Tabuchi).

0304-3940/$ – see front matter © 2014 Elsevier Ireland Ltd. All rights reserved.
http://dx.doi.org/10.1016/j.neulet.2013.12.063

2. Materials and methods

2.1. Animals

Postnatal days 3 (P3) to 5 (P5) Sprague-Dawley rats were used. All animal procedures were carried out according to the guidelines of the Laboratory Animal Research Center of Tsukuba University.

2.2. Reverse transcription-polymerase chain reaction (RT-PCR)

The cochlea, organ of Corti, and spiral ganglion were dissected. Total RNA was extracted from each cell, using Trizol (Invitrogen, Carlsbad, CA, USA). Reverse transcription was performed using total RNA (1 μg) with a GeneAmp PCR System 9600 (Perkin Elmer, Tokyo, Japan). The mRNA expression levels of $S1PR_{1-5}$ were detected by conventional RT-PCR with Taq polymerase (Takara, Shiga, Japan).

Glyceraldehyde-3-phoshate dehydrogenase (GAPDH) was used as an internal control for RNA integrity. S1PR primer sequences were as follows:

(1) $S1PR_1$-F: 5′-AGCGTTTGTCTGGAGAAGTACC-3′
$S1PR_1$-R: 5′-TAGCAAGGAGGCTGAAGACTGA-3′

(2) $S1PR_2$-F: 5′-CCTGAGAAGGTTCAGGAACACTAC-3′
$S1PR_2$-R: 5′-CCCAATGAGCATCAACATTCGAC-3′

(3) $S1PR_3$-F: 5′-ATGTCCGGTAGGAAGACGTTCA-3′
$S1PR_3$-R: 5′-AAGAAAGCACGCCGCATCTC-3′

(4) $S1PR_4$-F: 5′-GATCTTGGTGGCTTTTGTGG-3′
$S1PR_4$-R: 5′-CTCTCGCATCTTGAAGCTGA-3′

(5) $S1PR_5$-F: 5′-CCAGTGCACAAATGCCAA-3′
$S1PR_5$-R: 5′-GTTGTAGTGAAGGACGATGAC-3′

(6) GAPDH-F: 5′-AAGGTCATCCCAGAGCTGAA-3′
GAPDH-R: 5′-GTTGAAGTCACAGGAGACAACC-3′

2.3. Culture technique

The basal turn of the organ of Corti was dissected and cultured according to the methods of Van de Water and Ruben [16] and Sobkowicz et al. [17]. Cochlear explants were maintained in Dulbecco's modified Eagle's medium (DMEM) with 10% fetal bovine serum (FBS), 25 mM HEPES, and 30 U/mL penicillin. They were cultured in an incubator at 37 °C with 5% CO_2 at 95% humidity. Cochlear cultures were maintained in the above-described medium overnight (8–12 h) and then exposed to a medium containing 35 μM gentamicin for 48 h to assess the effects of S1PR antagonists [18,19]. Each S1PR antagonist was tested at concentrations of 1–100 μM.

2.4. S1P receptor antagonists

S1P and (R)-3-amino-(3-hexylphenylamino)-4-(oxobutyl-phosphonic) acid (W146, a selective $S1PR_1$ antagonist) and 1-[1,3-dimethyl-1-4-(2-methyllethyl)-1H-pyrazolo[3,4b]pyridin-6-yl]-4-(3,5-dichloro-4-pyridinyl)-semicar-bazide (JTE013, a selective $S1PR_2$ antagonist) were purchased from Sigma Japan (Tokyo, Japan). 2-Undecyl-thiazolidine-4-carboxylic acid (BML241, a selective $S1PR_3$ antagonist) was purchased from Cayman Chemical (Ann Arbor, MI, USA). W146 was initially dissolved in methanol to 10 mM and stored at −20 °C. JTE013 was initially dissolved in dimethyl sulfoxide (DMSO) to 10 mM and stored at −20 °C. BML241 was initially dissolved in dimethylformamide (DMF) to 10 mM and stored at −20 °C. Each antagonist was diluted in the culture medium to the final concentration immediately before use.

2.5. Cytochemistry

At the end of the tissue culture, the explants were fixed with 4% paraformaldehyde in phosphate-buffered saline (PBS) for 20 min and then permeabilized with 5% Triton X-100 (Sigma, St. Louis, MO, USA) in PBS with 10% fetal bovine serum (FBS) for 10 min. The specimens were stained with phalloidin with a conjugated Alexa Fluor probe (1:100, Molecular Probes, Carlsbad, CA, USA) at room temperature for 1 h. Phalloidin is a specific marker for cellular F-actin and labels stereociliary arrays and the cuticular plates of hair cells [12,18]. All experiments consisted of 8–20 explants per experimental group.

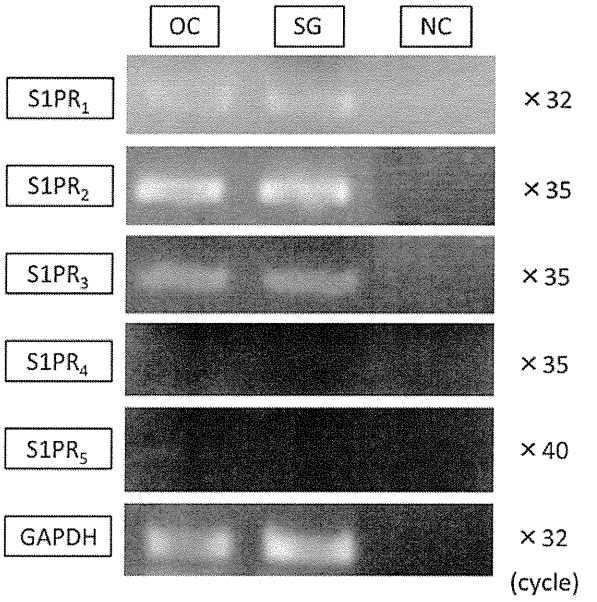

Fig. 1. Expression of S1PRs in the cochlea. RT-PCR analysis demonstrated that 3 S1P receptors ($S1P_{1-3}$) were expressed in the organ of Corti (OC) and spiral ganglion (SG) of Sprague-Dawley rats on postnatal days 3 (p3) to 5 (p5). However, the other 2 S1P receptors ($S1P_{4,5}$) were not detected. GAPDH primers served as a cDNA loading control (NC; negative control).

2.6. Assessment of cochlear hair cell damage

Hair cells were characterized as missing if no stereocilia or cuticular plates were observed by phalloidin staining. Quantitative results were obtained by evaluating 30 outer hair cells in a given microscopic field [15]. The average of 3 separate counts was used to represent each culture.

2.7. Western blot analysis

The organ of Corti and the spiral ganglion were homogenized in lysis buffer containing 0.25 M sucrose, 50 mM dithiothreitol, 3 mM HEPES (pH 7.9), 0.5 mM EGTA, 1 mM 4-(2-aminoethyl)-benzenesulfonyl fluoride, 0.8 mM aprotinin, 21 μM leupeptin, 36 μM bestatin, 15 μM pepstatin A, 14 μM (4-guanidino) butane, and 1% Triton X-100. After centrifugation (12,000×, 10 min, 4 °C), the supernatants were used for Western immunoblot analysis. Appropriate volumes of the samples (10 μg/lane), were mixed with equal volumes of sample buffer (100 mM Tris–HCl, PH 6.8, 4% SDS, 20% glycerol, 10% 2-mercaptoethanol, and 0.02% bromophenol blue), heated at 95 °C for 5 min, and then subjected to SDS–PAGE using 10% polyacrylamide gels. The proteins were transferred by semidry electroblotting from the gels to polyvinylidene difluoride membranes for 120 min. The blots were then blocked with the primary antibodies, cleaved caspase 9 or caspase 3 polyclonal antibody (Cell Signaling Technology, Denvers, MA, USA) for 18 h at 4 °C. Next, the blots were incubated with an appropriate second antibody, horseradish peroxidase-conjugated goat anti-rabbit IgG (Cell Signaling Technology), for 1 h. Immunoreactive bands

were visualized using enhanced chemiluminescence (ECL kit; GE Healthcare Japan, Tokyo, Japan). The scanned immunoblot images were densitometrically analyzed with an ImageQuant LAS4000 mini imager (GE Healthcare Japan, Tokyo, Japan). The result of each ratio of examined protein/β-actin protein was obtained from independent measurements ($n = 6$ per group for each measurement).

2.8. Data analysis

All data were expressed as the means ± SEMs. Statistical analysis was performed by unpaired t-tests or one-way analysis of variance (ANOVA) followed by Bonferroni post hoc tests, as required (StatView 5.0). Probability values less than 0.05 were considered significant.

3. Results

3.1. Expression of S1PRs in the cochlea

Nonquantitative RT-PCR analysis clearly detected $S1PR_2$ mRNA in the organ of Corti and spiral ganglion. $S1PR_1$ and $S1PR_3$ mRNA was also detected in both the organ of Corti and the spiral ganglion. In contrast to the results for $S1PR_{1-3}$, no expression of $S1PR_4$ or $S1PR_5$ mRNA was observed both in either the organ of Corti or the spiral ganglion (Fig. 1).

3.2. Effects of S1PR antagonists on cochlear hair cells (control study)

In control explants maintained in the initial medium for 48 h without exposure to gentamicin, almost all hair cells including 1 row of inner hair cells and 3 rows of outer hair cells were present (Fig. 2A). The effects of each antagonist and each solvent (W146, DMSO; JTE013, methanol; BML241, DMF) on the outer hair cells were examined and compared with the control explants. These antagonists and their solvents did not induce any significant outer hair cell loss when explants were cultured for 48 h in the medium containing these agents (data not shown).

3.3. Effects of S1PR antagonists on gentamicin ototoxicity

The effect of each antagonist on gentamicin-induced cochlear hair cell loss was examined using basal turn explants. The explants treated with gentamicin alone showed significantly reduced numbers of outer hair cells (Fig. 2A). Compared to the explants treated with gentamicin alone (the gentamicin control group), JTE013 increased the ratio of outer hair cell loss induced by gentamicin at the concentrations of 10 and 100 μM (Fig. 2A and B) (Bonferroni test: $p < 0.05$). The ratio of outer hair cell loss differed significantly between the 10 and 100 μM subgroups, suggesting the dose-dependency of outer hair cell damage within this range

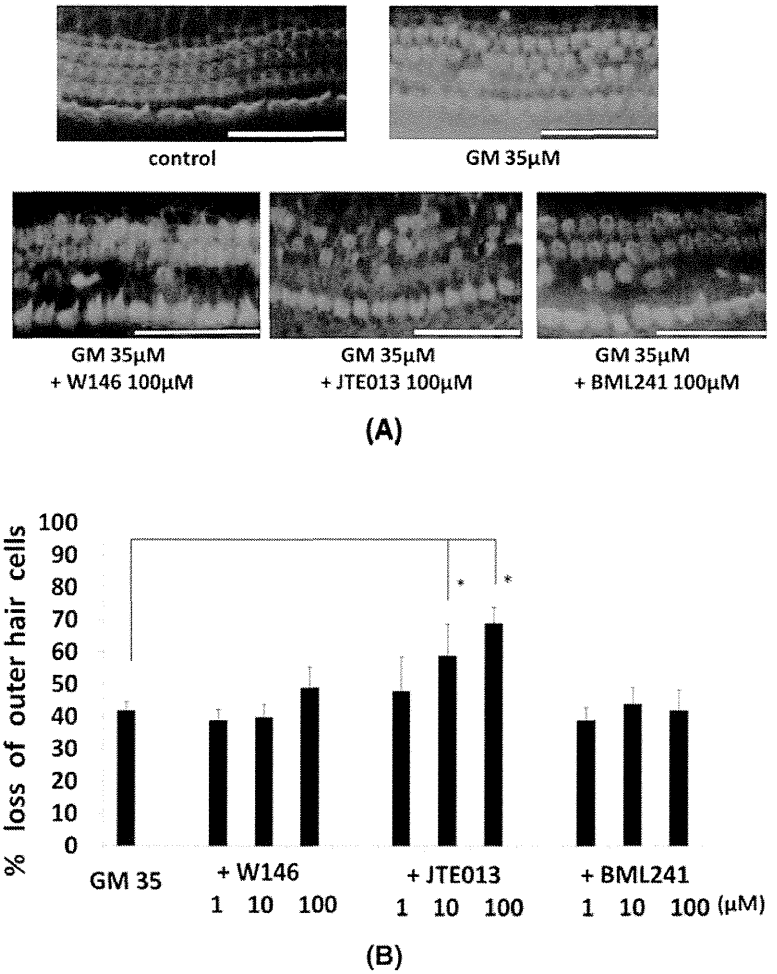

Fig. 2. Effects of $S1P_{1-3}$ antagonists on cochlear hair cells. The organ of Corti explant was cultured with or without gentamicin. (A) Representative microphotographs. (B) The effects of S1P antagonists on gentamicin ototoxicity were examined. The organ of Corti was cultured with 35 μM gentamicin alone or with 35 μM gentamicin plus 100 μM of each S1PR antagonist for 48 h. JTE013 (an $S1PR_2$ antagonist) increased hair cell loss at 10 and 100 μM as compared with the culture with gentamicin alone ($p < 0.05$, one-way ANOVA and Bonferroni test). Scale bar: 50 μm.

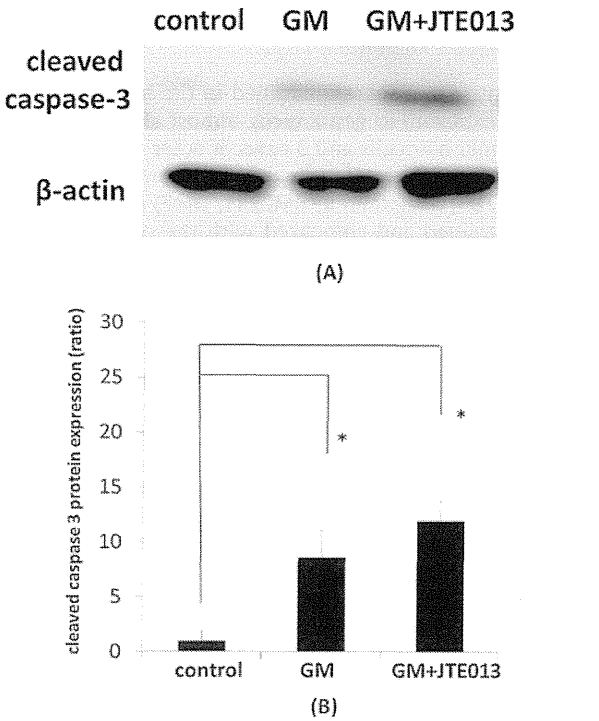

Fig. 3. Expression levels of cleaved caspase 3 in the organ of Corti were assessed by Western blot analysis ($n = 6$ in each group). (A) Typical blot images. β-Actin was used as an internal control. Cleaved caspase 3 was not detected in the control organ of Corti (without gentamicin). Cleaved caspase 3 was detected in the explant exposed to gentamicin. JTE013 increased expression levels of cleaved caspase 3. (B) Quantitative analysis of cleaved caspase-3. Control: tissue sample from organ of Corti maintained in the initial medium for 48 h. GM: organ of Corti treated with gentamicin 35 μM for 48 h. GM + JTE013: organ of Corti treated with 35 μM gentamicin plus 100 μM JTE013 for 48 h.

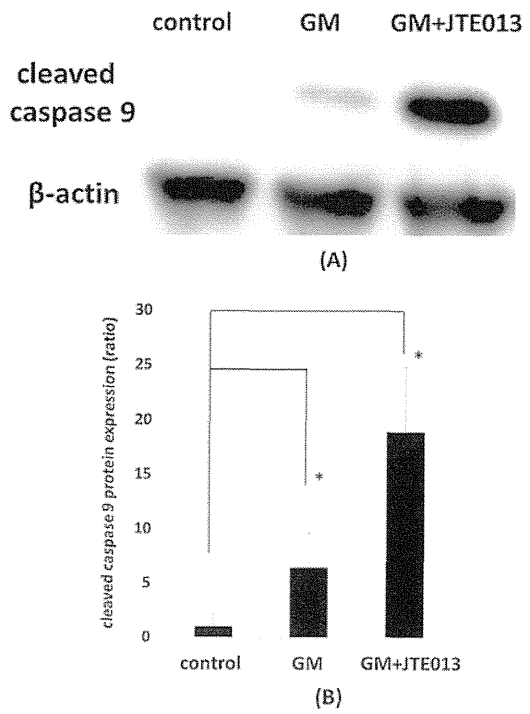

Fig. 4. Expression levels of cleaved caspase 9 were assessed by Western blotting. (A) Typical blot images. β-Actin was used as an internal control. Cleaved caspase 9 was not detected in the control organ of Corti (without gentamicin). Gentamicin induced cleaved caspase 9, and JTE further increased expression level of cleaved caspase-9. (B) Quantitative analysis of cleaved caspase-9. Control: tissue sample from the organ of Corti maintained in the initial medium for 48 h. GM: the organ of Corti treated with 35 μM gentamicin for 48 h. GM + JTE013: the organ of Corti treated with 35 μM gentamicin plus 100 μM JTE013 for 48 h.

of concentrations (Bonferroni test: $p < 0.05$). However, W146 (1, 10, and 100 μM) or BML241 (1, 10, and 100 μM) did not influence gentamicin ototoxicity (Fig. 2A and B).

3.4. Activation of the intrinsic apoptotic pathway in gentamicin ototoxicity

The protein expression levels of cleaved caspase-3 and cleaved caspase-9 in the cochlea were examined by Western blot analysis (Figs. 3 and 4). Neither cleaved caspase 3 nor cleaved caspase 9 was detected in the normal organ of Corti cultures (without gentamicin). Gentamicin induced expression of cleaved caspases 3 and 9. In addition, JTE013 treatment significantly increased expression levels of cleaved caspases 3 and 9 as compared with the gentamicin-alone group.

4. Discussion

Expression of $S1PR_{1-3}$ in the organ of Corti was shown in previous studies [10,11]. In the present study, we demonstrated that $S1PR_{1-3}$ mRNA was expressed in the spiral ganglion as well as in the organ of Corti of Sprague-Dawley rats'. However, $S1PR_4$ and $S1PR_5$ mRNA were not detected in the cochlea. The present findings seem reasonable because $S1PR_{1-3}$ are widely expressed in various tissues, whereas expression of $S1PR_4$ is reportedly limited to the lymphoid and hematopoietic tissues and that of $S1PR_5$ to the central nervous system [10,20].

On the basis of the results obtained for S1PR expression in the cochlea, we examined the effects of $S1PR_{1-3}$ antagonists on gentamicin ototoxicity. The results showed that the ratio of outer hair cell loss increased in the JTE013-treated group as compared with in the gentamicin-alone group. On the other hand, W146 or BML241 treatment had no effect on the gentamicin-induced damage of hair cells. S1P, produced intracellularly, generally functions as an anti-apoptotic substance. In our previous study, S1P protected hair cells against gentamicin ototoxicity [5]. The present findings strongly suggest that $S1PR_2$ signaling is important for cochlear hair cell survival in gentamicin ototoxicity. Kono et al. [10] and MacLennan et al. [21] recently reported that S1P signaling was essential for the maintenance of the cochlea in infantile animals via the activation $S1PR_2$. The $S1PR_2$-null mice were profoundly deaf, and the structure of the cochlea in $S1PR_2$ null mice was abnormal [10,21]. Their findings support our assumption that $S1PR_2$ signaling influences the fate of cochlear hair cells during gentamicin exposure.

The mechanisms of aminoglycoside-induced cochlear hair cell death are not fully known. However, it has been reported that the intrinsic apoptotic pathway is one of the major pathways leading to cochlear hair cell death [15,22]. We examined the activation of the intrinsic apoptotic pathway by measuring cleaved caspases 3 and 9. In agreement with the previous reports [15,22], gentamicin activated the intrinsic apoptotic pathway. Namely, both cleaved caspases 3 and cleaved caspases 9 were detected after gentamicin exposure. Furthermore, JTE013, an $S1PR_2$ antagonist, enhanced the cleavage of caspases 3 and 9 induced by gentamicin. On the basis of the present finding, it is assumed that S1P may inhibit the intrinsic apoptotic pathway via $S1PR_2$ in gentamicin ototoxicity.

5. Conclusions

An $S1PR_2$ antagonist enhanced the intrinsic apoptotic pathway of cochlear outer hair cells in gentamicin ototoxicity. This finding